CRYSTAL GROWTH & DESIGN

pubs.acs.org/crystal

Article

Modulating Organic/Inorganic Segregation in Columnar Mesophases

Estela de Domingo, Gregorio García, César L. Folcia, Josu Ortega, Jesús Etxebarria, and Silverio Coco*

Cite This: *Cryst. Growth Des.* 2023, 23, 6812−6821

Read Online

ACCESS | Metrics & More | Article Recommendations | Supporting Information

ABSTRACT: This work reports an uncommon modulation of columnar segregation of metal−organic triphenylene liquid crystals by blending two structurally dissimilar metallomesogens that can self-associate through complementary electron donor−acceptor interactions. The constituent molecules are *cis*-[$PtCl_2(CNR)_2$] (CNR = 2-(6-(4-isocyanophenoxy)hexyloxy)-3,6,7,10,11-pentakisdodecyloxytriphenylene) that displays an organic/inorganic segregated columnar mesophase and [$PtCl_2$(Bipy)] (Bipy = didodecyl 2,2′-bipyridyl-4,4′-dicarboxylate) that shows a lamellar mesomorphism. The phase diagram of this system was constructed using polarized optical microscopy (POM), differential scanning calorimetry (DSC), and X-ray scattering data. The phase diagram corresponds to a typical binary system with an intermediate compound (in this case a supramolecular aggregate) of stoichiometry [$PtCl_2(CNR)_2$]/2[$PtCl_2$(Bipy)], which is maintained in solution. This species shows an unusual columnar mesophase formed by the stacking of alternating organic/inorganic fragments. Quantum chemical calculations show that the columnar structure is mainly supported by complementary π electron donor−acceptor interactions between each triphenylene group of the isocyanide complex and a platinum-bipyridine molecule. This induces the elimination of the organic/inorganic columnar segregation of the isocyano parent component and constitutes an unconventional example of modulation of organic/inorganic segregation in columnar mesophases by the intercalation of metal complexes into hexaalkoxytriphenylene stacks.

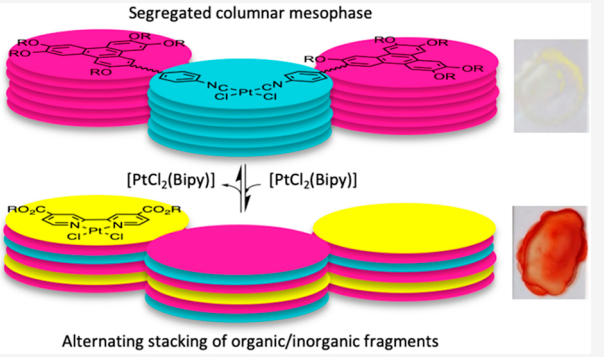

INTRODUCTION

Triphenylene-based discotic mesogens constitute a classical example of self-organized columnar materials[1−3] with interesting physical and chemical properties that make them suitable candidates for a number of applications including electrophotography,[4] electronics and optoelectronics,[5] LEDs,[6] chemical sensing,[7] and even for the preparation of birefringent films that improve the viewing angle of liquid crystal displays.[8]

Their properties are frequently related to their degree of structural organization. Therefore, understanding their dynamics and phase behavior at the molecular scale is fundamental for improved rational design. In this respect, chemical functionalization of the triphenylene core with different groups,[9−17] including metal−organic moieties,[18−24] has been extensively used to modulate the properties of these systems. There are also reports where the functionalization of the triphenylene is made at the end of one of the alkoxy substituents,[25] which can favor the formation of mesophases having segregated columns of different natures.[26−33] With metal−organic fragments, this is an easy way to produce hybrid organic/inorganic mesophases.[34−40]

Another possibility to tune the structural organization of liquid crystals is simply through the mixing of relatively simple components.[41−44] This approach is a useful alternative to the synthesis-intensive requirements needed for tuning the properties of single-component molecules and materials.[45−47] In fact, in most technological applications, the liquid crystalline material is not a pure substance, but it is a mixture of two or more species.

A well-studied type of columnar liquid crystal based on multicomponent systems is the case of aromatic donor−acceptor columnar liquid crystals fashioned from two different and complementary components, which self-assemble into alternating face-centered columnar structures, for example, binary mixtures of π-electron donating hexalkoxytriphenylene molecules and different π-electron acceptor partners such as naphthalene diimide,[43] mellitic triimide,[43] hexaazatriphenylenes,[48] or perylene-diimides.[49]

Liquid crystalline blends involving inorganic species have also been reported, but these studies are limited to a reduced number of cyclopalladated complexes,[50] salicylaldimato complexes,[51] *N*,*N*′-dialkylimidazolium tetrachlorometallate salts,[52]

Received: May 30, 2023
Revised: July 27, 2023
Published: August 18, 2023

alkene-platinum(II) compounds,[53] isocyanide-gold(I) derivatives,[54] dialkyl 2,2′-bipyridyl-4,4′-dicarboxylate complexes of Pt(II) and Pt(IV),[55] and some metal carboxylates.[56−60]

On these grounds and as a part of our continuing research program on feature modulation of columnar metallomesogens, here we have turned our attention to the use of mixtures for this purpose. We followed a simple strategy of studying the thermotropic behavior and phase diagram of a binary system composed of structurally dissimilar metallomesogens able to self-associate through complementary electron donor−acceptor interactions. The selection of the electron donating part (Scheme 1) follows from our previous studies, which

Scheme 1. Chemical Structures of $[PtCl_2(CNR_2)]$ and $[PtCl_2(Bipy)]$ Molecules

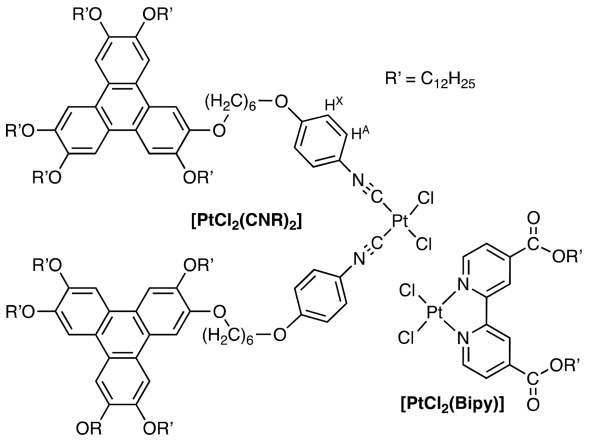

established that *cis*-$[PtCl_2(CNR)_2]$ (CNR = 2-(6-(4-isocyanophenoxy)hexyloxy)-3,6,7,10,11-pentakisdodecyloxytriphenylene) that bears the π-electron donating hexalkoxytriphenylene group (TPh) displays a hybrid organic/inorganic rectangular columnar mesophase with segregated columns of different natures.[37] As the electron acceptor partner, $[PtCl_2(Bipy)]$ (Bipy = didodecyl 2,2′-bipyridyl-4,4′-dicarboxylate) that shows a lamellar mesomorphism was chosen.[54]

We have found a rich mesomorphic behavior, which is dependent on the composition of the system. Self-assembly of $[PtCl_2(Bipy)]$ and $[PtCl_2(CNR)_2]$ in a 2:1 molar ratio results in the formation of an unusual columnar mesophase consisting of alternating stacking of organic/inorganic fragments. The columnar structure is mainly supported by complementary π electron donor−acceptor interactions between each triphenylene group of the isocyanide complex and a platinum-bipyridine molecule, which causes the elimination of the organic/inorganic columnar segregation of the isocyano parent component. In addition, quantum chemical calculations have also been performed to gain insight into the supramolecular self-assembled columnar structure at the molecular level. It is worth empathizing that the size of the model system here studied (616 atoms) and its complexity due to its metal−organic nature exceed common theoretical studies on liquid crystals.

RESULTS AND DISCUSSION

Synthesis. Literature methods were used for the synthesis of *cis*-$[PtCl_2(CNR)_2]$[37] and $[PtCl_2(Bipy)]$.[54] Both complexes were characterized spectroscopically, including $^{195}Pt\{^1H\}$ RMN spectra, which had not been previously reported (experimental section in the Supporting Information). The binary mixtures of pure compounds were prepared by dissolving the corresponding weights of the two compounds together in dichloromethane at ambient temperature and subsequently eliminating solvent under a vacuum.

Thermal Behavior and Self-Organization Properties. The phase diagram of this system has been constructed using polarized optical microscopy (POM), differential scanning calorimetry (DSC), and X-ray scattering data. Transition temperatures and thermal data are listed in Table 1 and Figure 1. The corresponding phase diagram is shown in Figure 2.

Table 1. Optical, Thermal, and Thermodynamic Data for Mixtures $[PtCl_2(Bipy)]/[PtCl_2(CNR)_2]$

mol % $[PtCl_2(CNR)_2]$	transition[a]	temperature[b] (°C)	ΔH[b] (kJ mol^{-1})
0	Cr → Cr'	32	8.6
	Cr' → Lam	81	7.2
	Lam → I	188	13.6
10	Cr + Col_{rec} → Cr' + Col_{rec}	35	5.0
	Cr' + Col_{rec} → Lam + I	82	5.1
	Lam → I	152	4.0
20	Cr + Col_{rec} → Cr' + Col_{rec}	34	1.0
	Cr' + Col_{rec} → Lam + I	80	2.5
	Lam + I → I	91	0.6
25	Cr + Col_{rec} → Cr' + Col_{rec}	40[c]	1.1[c]
	Cr' + Col_{rec} → Lam + I	78[c]	1.7[c]
	Lam + I → I	91[c]	1.2[c]
30	Cr + Col → Cr' + Col_{rec}	36	0.6
	Cr' + Col_{rec} → Col_{rec}+ I	}87	1.1[d]
	Col_{rec} + I → I		
33.3	Cr → Col_{rec}	−16	16.5
	Col_{rec} → I	97	2.7
35	Cr → Col_{rec*}	−16	14.5
	Col_{rec*} → I	100	2.3
40	Cr → Col_{rec*}	−10	20.0
	Col_{rec*} → I	110	4.5
50	Cr → Col_{rec*}	−6	24.2
	Col_{rec*} → I	109	6.7
60	Cr → Col_{rec*}	−4	27.9
	Col_{rec*} → I	103	7.9
70	Cr → Col_{rec}	−4	30.0
	Col_{rec*} → I	96	9.3
80	Cr → Col_{rec*}	−7	31.2
	Col_{rec*} → I	90	11.1
90	Cr → Col_{rec*}	−11	32.2
	Col_{rec*} → I	87	11.9
100	Cr → Col_{rec*}	−13	26.3
	Col_{rec*} → I	83	13.2

[a]Cr, Cr' crystal phases; Col_{rec}, rectangular columnar mesophase; Col_{rec*}, segregated rectangular columnar mesophase; Lam, lamellar mesophase; I, isotropic liquid. [b]Data collected from the second heating DSC cycle. [c]Data collected from the first heating DSC cycle. The transition temperatures are given as peak onsets. [d]Combined transitions. For mixtures with compositions lower than 33.3% in $[PtCl_2CNR_2]$, transitions below −15 °C have been omitted for clarity. All the DSC scans registered from −40 °C can be found in the Supporting Information.

https://doi.org/10.1021/acs.cgd.3c00660
Cryst. Growth Des. 2023, 23, 6812−6821

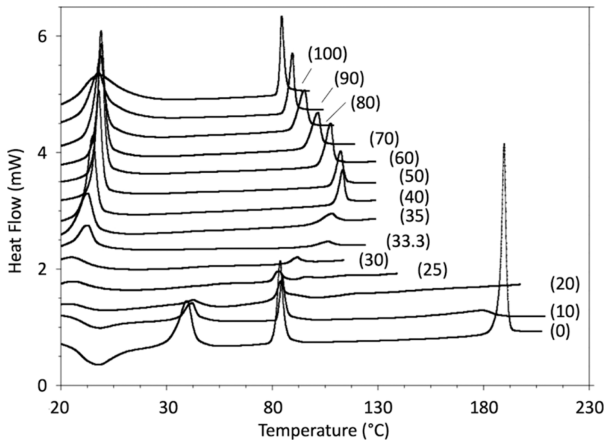

Figure 1. Heating DSC scans of the $[PtCl_2(Bipy)]/[PtCl_2(CNR)_2]$ mixtures. The compositions (mol % in $[PtCl_2(CNR)_2]$) are given in brackets.

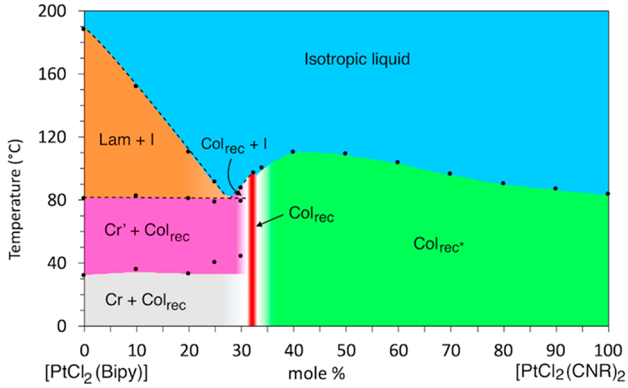

Figure 2. $[PtCl_2(Bipy)]/[PtCl_2(CNR)_2]$ phase diagram. The boundaries of the white regions could not be clearly determined. The temperatures given for the two-phase region Col_{rec} + I correspond to the beginning and end of the transition.

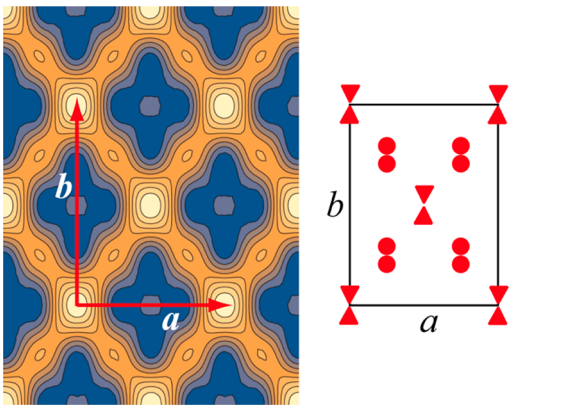

Figure 3. (Left) Electronic density map of the Col_{rec} phase of $[PtCl_2(CNR)_2]$ deduced from the X-ray powder diagram. The bright color corresponds to high-density regions. (Right) Scheme of the supramolecular organization in the mesophase. Red triangles and circles represent Pt moieties and triphenylene discs, respectively. The structure is built by stacking those elements at a distance of h in a perpendicular direction.

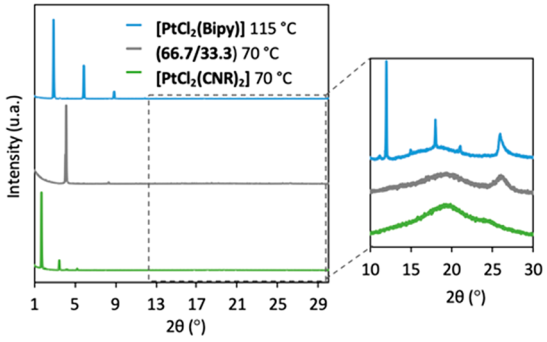

Figure 4. Diffraction patterns in the mesophase state of pure $[PtCl_2(Bipy)]$ (top); pure $[PtCl_2(CNR)_2]$ (bottom); 33.3% composition in $[PtCl_2(CNR)_2]$ (middle).

The parent 2,2′-bipyridine compound shows a lamellar (Lam) mesophase and crystal-to-crystal transitions before melting,[54] while the isocyano-triphenylene derivative displays a rectangular columnar (Col_{rec*}) mesophase, where triphenylene cores and platinum moieties are segregated into different columnar units.[37]

Figure 3 shows the electronic density map of $[PtCl_2(CNR)_2]$ as derived by considering just the 2 most intense peaks of the X-ray powder diagram (green curve in Figure 4). A detailed description of the procedure for obtaining the density map can be found in the Supporting Information and ref 61. The unit cell parameters are a = 63 Å and b = 85 Å.[37] In the map we can identify the most intense maxima with the metallic fragments, while the secondary maxima must correspond to the triphenylenes. Each principal maximum contains 2 adjacent Pt moieties. In this way, and according to ref 37, each unit cell has 4 Pt atoms and 8 triphenylene discs (the number of molecular units is Z = 4). The structure presents an arrangement in segregated columns of different natures (inorganic and organic) in a conventional fashion. Figure 3 also shows a schematic representation of the supramolecular organization of the complex, as suggested by the electronic density map. The structure is formed by stacking the elements drawn at a distance h = 3.5 Å in a direction perpendicular to the paper. This stacking periodicity is deduced from the position of the peak in the wide-angle region ($2\theta \approx 25°$), as shown in the right-most diagram of Figure 4. The mass density ρ is given by $4M/V$, where M is the molecular mass of the complex (2996 u) and $V = abh$. It turns out ρ = 1.06 g/cm^3, which is a reasonable value, supporting the consistency of the proposed model.

The mixture with compositions of 66.7% $[PtCl_2(Bipy)]$/33.3% $[PtCl_2(CNR)_2]$, which correspond to an intermediate compound (see below), divides the diagram into two self-contained zones. For concentrations lower than 33.3% in $[PtCl_2(CNR)_2]$, the parent components are immiscible, and only two-phase areas are observed. In contrast, for higher compositions, there is a total miscibility. Consequently, only a single-phase region appears. In the isotropic liquid, at higher temperatures, the system shows a single liquid phase over the entire range of compositions.

The intermediate compound displays enantiotropic mesomorphism from −16 to 87 °C. The texture observed by POM on cooling from the isotropic liquid shows a mosaic-like texture (Figure 5), similar to that of the pure $[PtCl_2(CNR)_2]$. However, the diffraction pattern of this species is different from those of both pure components, the isocyanide complex and the bipyridyl derivative (Figure 4), which reveals their different natures.

https://doi.org/10.1021/acs.cgd.3c00660
Cryst. Growth Des. 2023, 23, 6812−6821

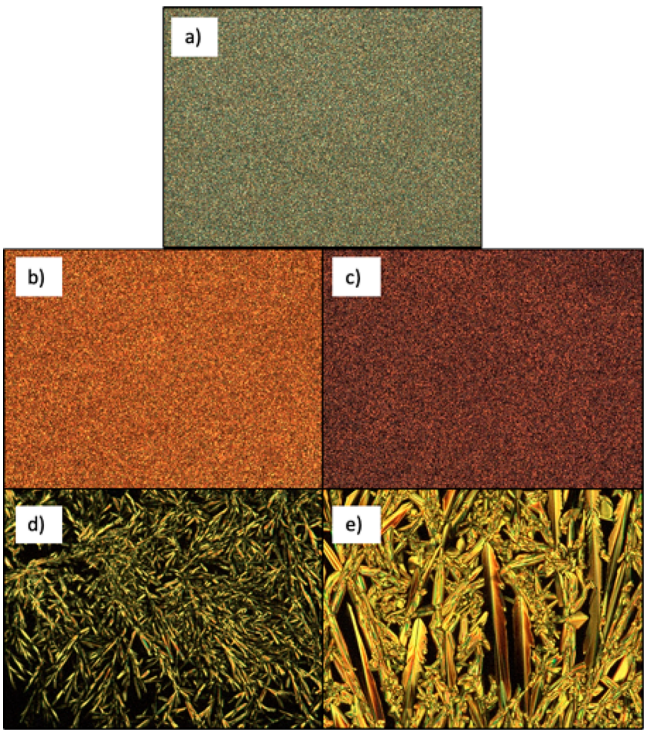

Figure 5. Optical polarizing microscopy photographs (×100, crossed polarizers) on cooling from the isotropic phase of (a) pure $[PtCl_2(CNR)_2]$ at 70 °C; (b) 50% $[PtCl_2(Bipy)]$/50% $[PtCl_2(CNR)_2]$ at 75 °C; (c) 66.7% $[PtCl_2(Bipy)]$/33.3% $[PtCl_2(CNR)_2]$ at 70 °C; (d) 90% $[PtCl_2(Bipy)]$/10% $[PtCl_2(CNR)_2]$ at 145 °C; and (e) pure $[PtCl_2(Bipy)]$ at 175 °C.

In the small-angle region two peaks are essentially observed, the second at twice the angle of the first (gray curve in Figure 4). This greatly contrasts with the X-ray patterns found for typical columnar phases, where the angular positions of the most prominent peaks do not bear a simple relationship. It is interesting to note the remarkable displacement of the main first peak toward larger angles in relation to that observed in $[PtCl_2(CNR)_2]$, which suggests a much smaller unit cell in this case. Given the similarity of the two optical textures (Figure 5) we also propose a Colrec phase for the mixture. Identifying the observed peaks with reflections (11) and (22) the density map shown in Figure 6 is obtained. This assignment implies a correct mass density for the structure as will be shown below. The plane group has *c2mm* symmetry, like $[PtCl_2(CNR)_2]$. In this case, however, in contrast to the pure complex, the primary and secondary maxima of the electronic density cannot be distinguished from each other but are all the same size. Consequently, each maximum must contain all possible elements with high electronic density, that is, Pt atoms from $[PtCl_2(CNR)_2]$, triphenylene units, and bipyridine units (which, in their turn, have associated their own Pt atoms). All of these elements must stack together to conform the high-density regions. This kind of "hybrid" organization implies an unusual molecular rearrangement in which the inorganic–organic columnar segregation of the parent $[PtCl_2(CNR)_2]$ compound has completely disappeared. Given the chemical composition of the mixture, the content of each stack must be composed by 5 objects: one metallic fragment from $[PtCl_2(CNR)_2]$, two triphenylene discs, and two $[PtCl_2(Bipy)]$ units. Presumably this association is stabilized through strong interactions between triphenylene and

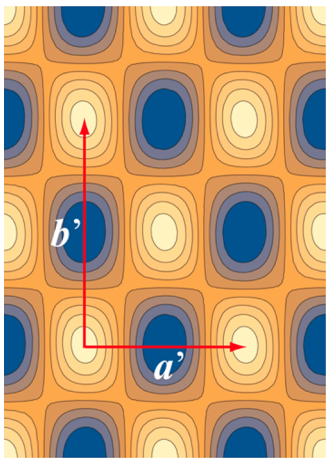

Figure 6. Electronic density map of the mixture $[PtCl_2(CNR)_2]$/2$[PtCl_2(Bipy)]$ obtained from the X-ray powder diagram. Bright color corresponds to high-density regions.

bipyridine moieties, as will be shown later. The stacking distance is in this case h' = 3.4 Å, as deduced from the position of the peak at $2\theta \approx 26°$ (diagram on the right in Figure 4). Since there are two columns per unit cell, the mass density is given by $\rho = 2(M + 2M')/(a'b'5h')$, where M' = 846 u is the molecular mass of $[PtCl_2(Bipy)]$, and a',b' are the unit cell parameters. A density ρ = 1.0 g/cm^3 results for a' = 26 Å, b' = 35 Å, which fit the observed (11) and (22) peaks quite well.

Regarding the mixtures with compositions lower than 33.3% in $[PtCl_2(CNR)_2]$, the solid obtained from cooling a molten mixture shows clearly the sum of the diffraction patterns of the bipyridyl derivative and the intermediate compound just described, proving that the solid is a mixture of both components. When the mixed solid is heated, two regions of partial melting or clearing appear on the diagram, and mixtures of the end-member phases (Cr or Cr' + Col_{rec} and Lam + I) are observed (Figure 2). Finally, the sample becomes an isotropic liquid. In agreement with the power X-ray data, the clearing point appears in the DSC scans as two endothermic peaks revealing a simple eutectic system (Figure 1), the one at lower temperature corresponding to the partial clearing (eutectic temperature), and the second one, which appears as a broad signal corresponding to the transition from the two-phase region to isotropic liquid.

For compositions of $[PtCl_2(CNR)_2]$ above 33.3%, only single-phase areas are observed, and the DCS scans show fairly sharp peaks. These observations are consistent with a solid solution, which melts to give a rectangular columnar mesophase with temperature range, texture, and diffraction patterns (Figure 8) similar to those of the $[PtCl_2(CNR)_2]$ complex (Figures 1, 5, and 8).

Solution Characterization of Donor–Acceptor Interactions. While both individual components are off-white or yellow, the formation of mixtures resulted in the appearance of an intense red color. The UV–vis spectra of thin films show a broad absorption band centered at 520 nm, which is not observed in the pure isolated complexes; a representative example is gathered in Figure 9.

This result suggests the formation of supramolecular aggregates through charge-transfer (CT) interactions between electron donor (TPh)–acceptor (Bipy) pairs, as reported for related systems.[47] In dichloromethane solution, the UV/vis absorption spectra of all the mixtures are very similar,

https://doi.org/10.1021/acs.cgd.3c00660
Cryst. Growth Des. 2023, 23, 6812–6821

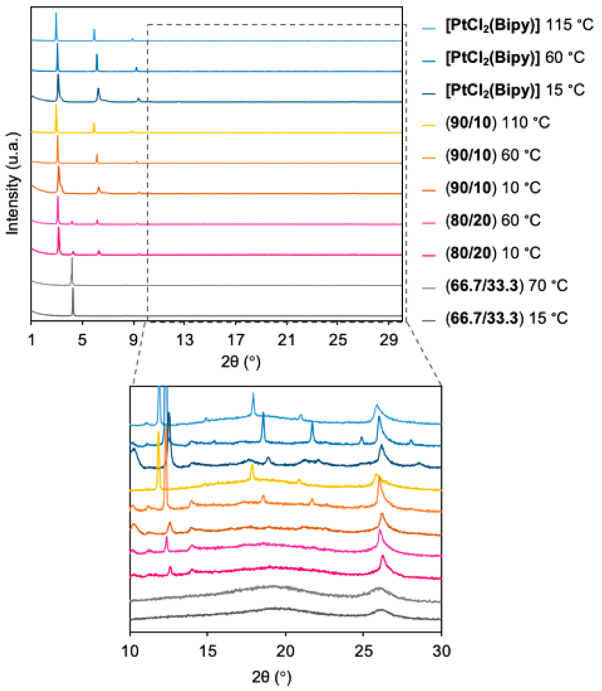

Figure 7. Diffraction patterns of $[PtCl_2(Bipy)]$ and some mixtures with high content of the bipyridine component at different temperatures. From top to bottom: pure $[PtCl_2(Bipy)]$ at 115 °C (Lam), 60 °C (Cr') and 15 °C (Cr); 90% $[PtCl_2(Bipy)]$/10% $[PtCl_2(CNR)_2]$ at 110 °C (Lam + I), 60 °C (Cr' + Col_{rec}) and 10 °C (Cr + Col_{rec}); 80% $[PtCl_2(Bipy)]$/20% $[PtCl_2(CNR)_2]$ at 60° (Cr' + Col_{rec}) and 10 °C (Cr + Col_{rec}); 66.7% $[PtCl_2(Bipy)]$/33.3% $[PtCl_2(CNR)_2]$ at 70 and 15 °C (Col_{rec}).

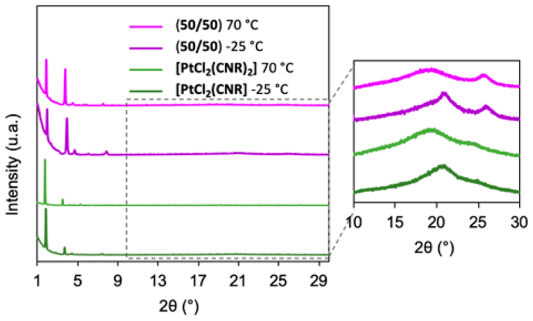

Figure 8. Diffraction patterns of pure $[PtCl_2(CNR)_2]$ and a 1:1 mixture at different temperatures. From top to bottom: 50% composition at 70 °C (Col_{rec*}) and −25 °C (Cr); pure $[PtCl_2(CNR)_2]$ at 70 °C (Col_{rec*}) and −25 °C (Cr).

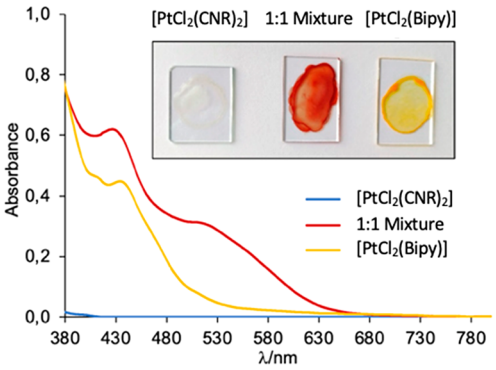

Figure 9. UV−vis absorption spectra and photographic images of thin films of $[PtCl_2(CNR)_2]$, $[PtCl_2(Bipy)]$, and a 1:1 mixture.

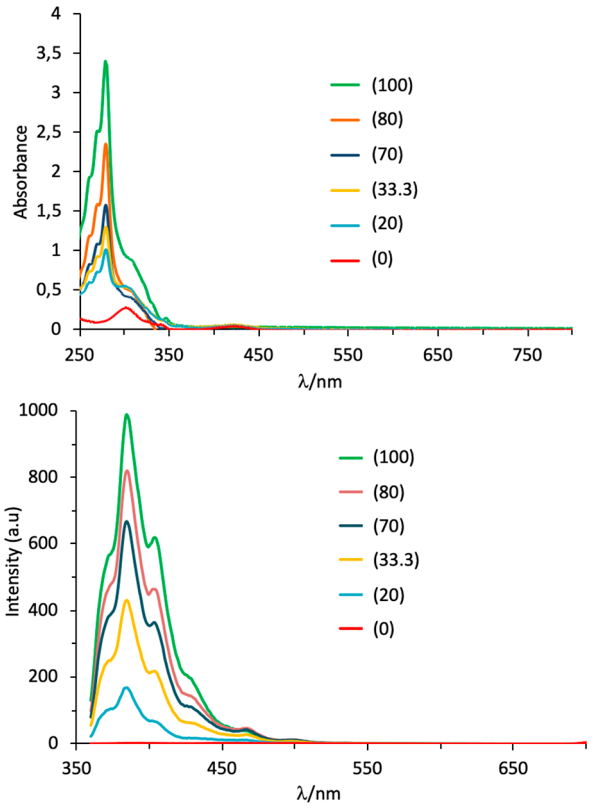

Figure 10. UV−vis absorption (top) and luminescence emission (bottom, λ_{exc} = 340 nm) spectra (CH_2Cl_2, 10^{-5} M) of the $[PtCl_2(Bipy)]$/$[PtCl_2(CNR)_2]$ mixtures. The compositions (mol % in $[PtCl_2(CNR)_2]$) are given in brackets.

displaying the structured spectral pattern characteristic of the isocyano complex $[PtCl_2(CNR)_2]$ (Figure 10).[37] Note that the characteristic absorptions of the bipyridyl component present in the mixture are not observed,[62] due to their overlap with the most intense bands of the triphenylene-isocyanide complex.

In the case of the mixtures, in dichloromethane solution, all of them are luminescent, showing the same emission spectrum as that of the $[PtCl_2(CNR)_2]$ complex (Figure 10). Thus, under these conditions, *the components of* the mixture should not interact strongly at the molecular level.

In the solid state, luminescence is observed only for compositions lower than 33.3% in $[PtCl_2(CNR)_2]$ (Figure 11). These mixtures display the characteristic phosphorescent emission of the bipyridyl component, which decreases as the percentage of the isocyano complex increases. The emission is completely lost for 33.3% composition in $[PtCl_2(CNR)_2]$. These results are consistent with the two-phase regions observed in the phase diagram for concentrations lower than 33.3%.

In contrast to the behavior observed in dichloromethane solution, ^{1}H NMR titration of $[PtCl_2(CNR)_2]$ (10^{-2} M) with $[PtCl_2(Bipy)]$) in C_6D_6 showed a clear shift of some aromatic signals (Figure 12), indicating supramolecular association between both complexes through interactions involving the triphenylene and bipyridine moieties. Plotting the experimental displacements and fitting the points to appropriate models gave a good estimation from a 1:2 full model (Figure 13),[63−65] affording complexation constants: K_1 = 7520 (±236) and K_2 =

https://doi.org/10.1021/acs.cgd.3c00660
Cryst. Growth Des. 2023, 23, 6812−6821

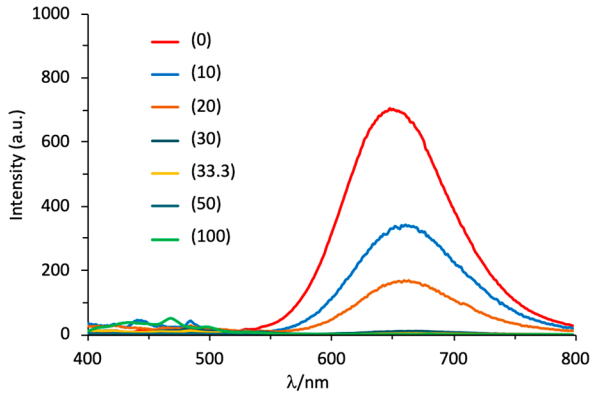

Figure 11. Luminescence emission spectra in the solid state of the $[PtCl_2(Bipy)]/[PtCl_2(CNR)_2]$ mixtures (λ_{exc} = 350 nm). The compositions (mol % in $[PtCl_2(CNR)_2]$) are given in brackets.

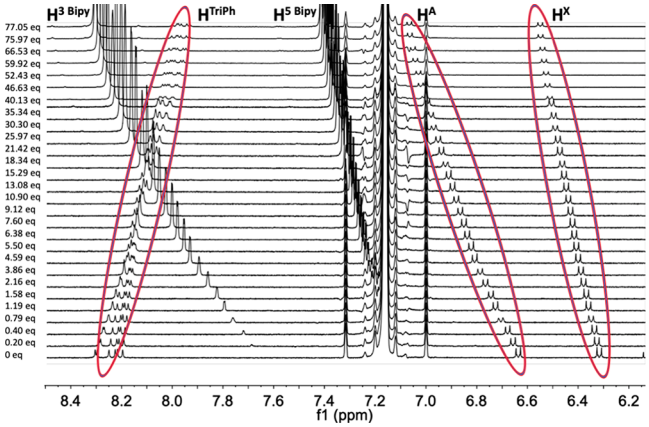

Figure 12. ^{1}H NMR titration of $[PtCl_2(CNR)_2]$ with $[PtCl_2(Bipy)]$ in C_6D_6. The spectra were recorded by using a constant concentration of $[PtCl_2(CN\text{-}TPh)_2]$ (10^{-2} M) at 298 K.

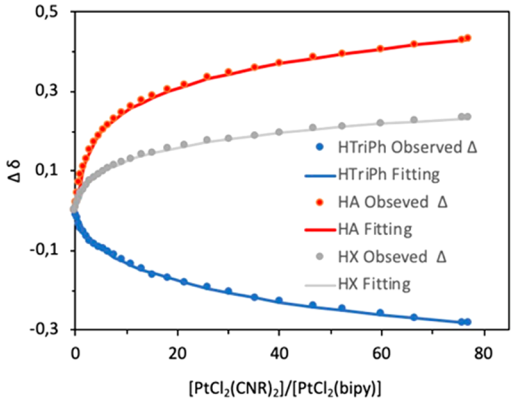

Figure 13. ^{1}H NMR titration plots and curve fittings of $[PtCl_2(CNR)_2]$ and $[PtCl_2(Bipy)]$ in benzene-d_6, H^{TriPh} (8.24 → 7.96 ppm), and H^A and H^X signals.

218 (±3), thus confirming the stoichiometry of the intermediate compound found in the solid state (see the Supporting Information for details).

Moreover, concentration-dependent experiments for the $[PtCl_2(CNR)_2]/2[PtCl_2(Bipy)]$ composition carried out by ^{1}H NMR spectroscopy in C_6D_6 show that the shift of the aromatic signals of the mixture with respect to those of the individual components progressively decreases with increasing dilution (Figure 14). This result reveals that for a concentration of 10^{-4} M, the components would not aggregate but would coexist independently.

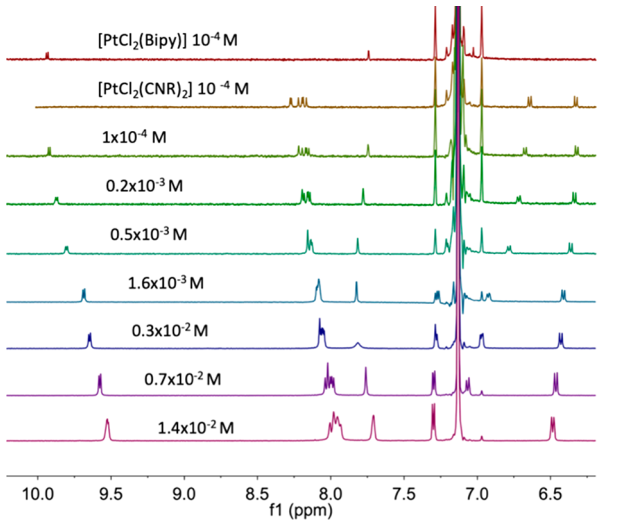

Figure 14. ^{1}H NMR of $[PtCl_2(CNR)_2]/2[PtCl_2(Bipy)]$ in benzene-d_6 at different concentrations.

Quantum Chemical Calculations. In order to gain a deeper insight into the columnar structure at the molecular level of the $[PtCl_2(CNR)_2]/2[PtCl_2(Bipy)]$ mixture, the supramolecular aggregate (or cluster) of this system, whose construction is based on the X-ray powder diffraction data, was studied by using density functional tight-binding calculations (see the theoretical section in the Supporting Information for a more detailed description).[66]

The minimum-energy structure calculated for the cluster model is constituted by the stacking of TPh discs (blue in Figure 15), Pt fragments from $[PtCl_2(CNR)_2]$ (red), and

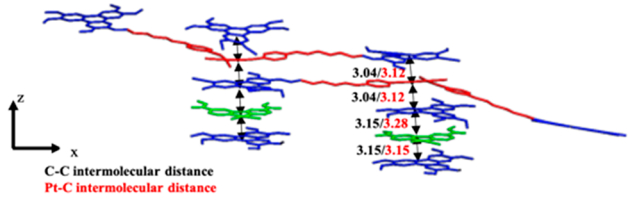

Figure 15. Side view of the stacking model calculated by the GFN2-xTB xTB tight-binding method for the columnar arrangement of the $[PtCl_2(CNR)_2]/2[PtCl_2(Bipy)]$ mixture. Color code: Pt moieties from $[PtCl_2(CNR)_2]$, red; $[PtCl_2(Bipy)]$ molecules, green; TPh fragments, blue. Hydrogen atoms are omitted. The shortest distances between metallic and TPh fragments are also displayed. Units are in Å.

$[PtCl_2(Bipy)]$ units (green). For some TPh fragments, we have considered the complete $[PtCl_2(CNR)_2]$ molecule in order to show the cross-linked effect between columns. This structure results in stacking distances of approximately 3.17 Å, in agreement with experimental data. In this respect, it must be mentioned that the slightly different stacking distances shown in Figure 15 should not be considered as experimentally distinguishable. Note that the supramolecular cluster displayed in Figure 15 does not correspond to the stoichiometric

https://doi.org/10.1021/acs.cgd.3c00660
Cryst. Growth Des. 2023, 23, 6812−6821

composition, but it represents the short-range structure where each Pt fragment is sandwiched between two TPh discs.

Figure 16 collects interaction energies computed for the supramolecular structure describing the columnar phase of the

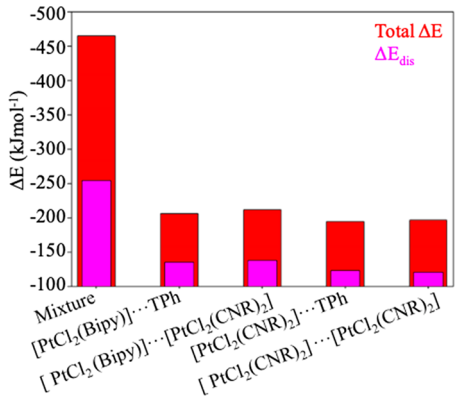

Figure 16. Calculated iteration energies (ΔE) for the $[PtCl_2(CNR)_2]/2[PtCl_2(Bipy)]$ mixture.

$[PtCl_2(CNR)_2]/2[PtCl_2(Bipy)]$ mixture. The total interaction energy has been calculated as the change in the energy of the respective units, referring to the number of interacting Pt atoms with TPh fragments. ΔE yields a value of −465.2 kJ·mol^{-1} (−697.9 kJ·mol^{-1} refers to the number of $[PtCl_2(CNR)_2]$ molecules). In this case, ΔE has been decomposed as the sum of the interaction energy between different fragments: $[PtCl_2(BiPy)]\cdots TPh$ and $[PtCl_2(CNR)_2]\cdots TPh$. Both $[PtCl_2(BiPy)]\cdots TPh$ and $[PtCl_2(CNR)_2]\cdots TPh$ terms contribute similarly to the ΔE (−201.2 kJ·mol^{-1}). The contribution from the dispersion energy (ΔE_{dis}) represents only 54.7% to the total ΔE. As seen below, charge transfer interactions play a key role in the stabilization of the columnar phase of the $[PtCl_2(CNR)_2]/2[PtCl_2(Bipy)]$ mixture.

Aimed at obtaining information into the nature of the donor−acceptor interactions, we have assessed the charge distribution, through the electrostatic potential plots (ESP) in the supramolecular cluster here optimized as the changes with respect to the constituent molecules (Figure 17).

The ESP plot of $[PtCl_2(Bipy)]$ reveals a centralized distribution of negative charges (Red) across the Bipy motif, while positive charges (Blue) are around the Pt atoms. On the other hand, the ESP plot of $[PtCl_2(CNR)_2]$ shows that relative positive charges are localized within the center of the TPh core as well over Pt atoms, while the (isocyanophenoxy)hexyloxy regions hold most of the negative charges. As a matter of fact, the optimized structure for the $[PtCl_2(CNR)_2]/2$-$[PtCl_2(Bipy)]$ mixture indicated a face-to-face overlap between Bipy or isocyanophenoxy motifs and TPh aromatic planes with an eclipsed geometry. Such configuration allows that the Pt moiety with a positive charge distribution be located over the edge of TPh cores, which indicates a negative charge distribution.

Finally, further analysis of the intermolecular interactions has been carried out considering reduced density gradient (RDG) isosurfaces to display the strength and nature of the intermolecular interactions (Figure 18).[67] Green RDG isosurfaces are observed between TPh motifs and Pt organometallic regions (for both $[PtCl_2(CNR)_2]$ or $[PtCl_2(Bipy)]$), indicating van der Waals interactions between the TPh core and aromatic

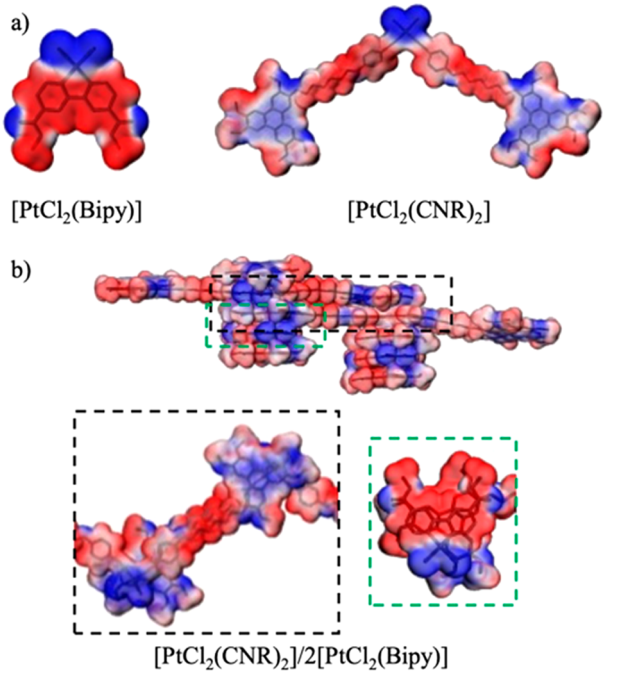

Figure 17. ESP plots of (a) $[PtCl_2(Bipy)]$ and $[PtCl_2(CNR)_2]$ molecules; (b) $[PtCl_2(CNR)_2]/2[PtCl_2(Bipy)]$ cluster (side and upper views). For the sake of clarity, only $PtCl_2\cdots TPh$ regions are highlighted for the $[PtCl_2(CNR)_2]/2[PtCl_2(Bipy)]$ mixture. Red and blue colors indicate the lowest and highest ESP. Hydrogen atoms are omitted.

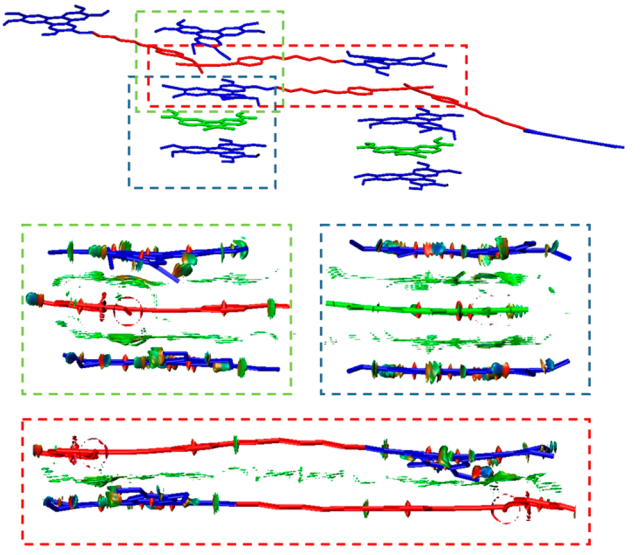

Figure 18. RDG isosurfaces of $[PtCl_2(CNR)_2]/2[PtCl_2(Bipy)]$ (with special interest in $PtCl_2\cdots TPh$ interacting regions). RDG green color points out attractive interactions. Hydrogens atoms are omitted.

regions around the Pt atoms (i.e., Bipy or isocyanophenoxy motifs) and strong attractive interactions between Pt−Cl regions and TPh edges, respectively.

CONCLUSIONS

This study shows that the use of liquid crystalline blends is a simple and useful strategy to modulate the features of columnar mesophases of triphenylene-derived metallomesogens. The mixture of two platinum(II) complexes, the

https://doi.org/10.1021/acs.cgd.3c00660
Cryst. Growth Des. 2023, 23, 6812−6821

isocyano-triphenylene derivative $[PtCl_2(CNR)_2]$ that displays an organic/inorganic segregated columnar mesophase, and $[PtCl_2(Bipy)]$ (Bipy = didodecyl 2,2′-bipyridyl-4,4′-dicarboxylate) that shows a lamellar mesomorphism, gives rise to an interesting mesomorphic behavior. For concentrations lower than 33.3% in $[PtCl_2(CNR)_2]$, the parent components are immiscible, and only two-phase areas corresponding to a eutectic system are observed before clearing. In contrast, for higher compositions, there is total miscibility, giving a segregated columnar mesophase with a similar structure to that of the isocyanide disk-like component but with wider temperature ranges. The most remarkable result is the formation of an intermediate supramolecular complex of stoichiometry $[PtCl_2(CNR)_2]/2[PtCl_2(Bipy)]$, which divides the phase diagram into two independent parts. This aggregate displays a columnar mesophase that is different from those of both pure components, whose structure is constituted by the stacking of alternating organic/inorganic fragments. Quantum chemical calculations, in accordance with UV−vis and ^1H NMR data, show that the formation of this columnar structure is supported by π electron donor−acceptor interactions between each triphenylene group of the isocyanide complex and a platinum-bipyridine molecule.

These results show clearly that the formation of the intermediate supramolecular complex through donor−acceptor interactions produces the breaking of the organic/inorganic columnar segregation of the isocyano parent component to give a stacking of alternating organic/inorganic moieties. This constitutes an unconventional example of modulation of organic/inorganic segregation in columnar mesophases by intercalation of platinum(II) complexes into hexaalkoxytriphenylene stacks.

This approach can provide a useful alternative to property modulation by chemical functionalization, for future tailoring of metal−organic liquid crystals.

■ ASSOCIATED CONTENT

Supporting Information

The Supporting Information is available free of charge at https://pubs.acs.org/doi/10.1021/acs.cgd.3c00660.

Materials and methods, full details of synthetic methods, spectroscopic data for the compounds, and DSC thermograms not included in the text (PDF)

■ AUTHOR INFORMATION

Corresponding Author

Silverio Coco − *IU CINQUIMA/Química Inorgánica, Facultad de Ciencias, Universidad de Valladolid, 47011 Valladolid, Castillay León, Spain;* orcid.org/0000-0002-8959-1075; Email: silverio.coco@uva.es

Authors

Estela de Domingo − *IU CINQUIMA/Química Inorgánica, Facultad de Ciencias, Universidad de Valladolid, 47011 Valladolid, Castillay León, Spain*

Gregorio García − *IU CINQUIMA/Química Inorgánica, Facultad de Ciencias, Universidad de Valladolid, 47011 Valladolid, Castillay León, Spain;* orcid.org/0000-0003-3200-3153

César L. Folcia − *Department of Physics, University of the Basque Conuntry, UPV/EHU, 48080 Bilbao, Spain;* orcid.org/0000-0003-2607-2937

Josu Ortega − *Department of Physics, University of the Basque Conuntry, UPV/EHU, 48080 Bilbao, Spain*

Jesús Etxebarria − *Department of Physics, University of the Basque Conuntry, UPV/EHU, 48080 Bilbao, Spain;* orcid.org/0000-0002-3948-6779

Complete contact information is available at: https://pubs.acs.org/10.1021/acs.cgd.3c00660

Author Contributions

The authors have contributed equally to the paper.

Notes

The authors declare no competing financial interest.

■ ACKNOWLEDGMENTS

This work was sponsored by the Ministerio de Ciencia e Innovación (Project PID2020-118547GB-I00), the Junta de Castilla y León (Project VA224P20), and the Basque Government (Project IT1458-22). E.D. thanks MECD for a FPU grant. The authors thankfully acknowledge the computer resources at Lusitania II and CIERZO-CAESARAUGUSTA III and the Technical support provided by Cénits-COMPUTAEX (FI-2022-1-0009, FI-2022-3-0008), Centro de Supercomputación de Aragón (QHS-2023-3-0005, QH-2023-1-0002) and Red Española de Supercomputación. We thank Dr. S. Ferrero (University of Valladolid) for his help in the NMR titration experiments.

■ REFERENCES

(1) Kumar, S. Self-organization of disc-like molecules: chemical aspects. *Chem. Soc. Rev.* **2006**, *35*, 83−109.

(2) Pal, S. K.; Setia, S.; Avinash, B. S.; Kumar, S. Triphenylene-based discotic liquid crystals: recent advances. *Liq. Cryst.* **2013**, *40*, 1769−1816.

(3) Wohrle, T.; Wurzbach, I.; Kirres, J.; Kostidou, A.; Kapernaum, N.; Litterscheidt, J.; Haenle, J. C.; Staffeld, P.; Baro, A.; Giesselmann, F.; Laschat, S. Discotic liquid crystals. *Chem. Rev.* **2016**, *116*, 1139−1241.

(4) Adam, D.; Schuhmacher, P.; Simmerer, J.; Haussling, L.; Siemensmeyer, K.; Etzbachi, K. H.; Ringsdorf, H.; Haarer, G. Fast photoconduction in the highly ordered columnar phase of a discotic liquid cristal. *Nature* **1994**, *371*, 141−143.

(5) Zhang, L.; Hughes, D. L.; Cammidge, A. N. Discotic Triphenylene Twins Linked through Thiophene Bridges: Controlling Nematic Behavior in an Intriguing Class of Functional Organic Materials. *J. Org. Chem.* **2012**, *77*, 4288−4297.

(6) Gupta, M.; Pal, S. K. Triphenylene-Based Room-Temperature Discotic Liquid Crystals: A New Class of Blue-Light-Emitting Materials with Long-Range Columnar Self-Assembly. *Langmuir* **2016**, *32*, 1120−1126.

(7) Bhalla, V.; Singh, H.; Kumar, M.; Prasad, S. K. Triazole-Modified Triphenylene Derivative: Self-Assembly and Sensing Applications. *Langmuir* **2011**, *27*, 15275−15281.

(8) Mori, H.; Itoh, Y.; Nishiura, Y.; Nakamura, T.; Shinagawa, Y. Performance of a novel optical compensation film ased on negative birefringence of discotic compound for wide-viewing-angle twisted-nematic liquid-crystal displays. *Jpn. J. Appl. Phys.* **1997**, *36* (1A), 143−147.

(9) Boden, N.; Bushby, R. J.; Cammidge, A. N. Functionalization of discotic liquid crystals by direct substitution into the discogen ring: α-nitration of triphenylene-based discogens. *Liq. Cryst.* **1995**, *18*, 673−676.

(10) Boden, N.; Bushby, R. J.; Cammidge, A. N.; Headdock, G. Novel discotic liquid crystals created by electrophilic aromatic substitution. *J. Mater. Chem.* **1995**, *5*, 2275−2281.

(11) Kumar, S.; Manickam, M.; Balagurusamy, V. S. K.; Schonherr, H. Electrophilic aromatic substitution in triphenylene discotics: synthesis of alkoxynitrotriphenylenes. *Liq. Cryst.* **1999**, *26*, 1455−1466.
(12) Bushby, R. J.; Boden, N.; Kilner, C. A.; Lozman, O. R.; Lu, Z.; Liu, Q.; Thornton-Pett, M. A. Helical geometry and liquid crystalline properties of 2,3,6,7,10,11-hexaalkoxy-1-nitrotriphenylenes. *J. Mater. Chem.* **2003**, *13*, 470−474.
(13) Boden, N.; Bushby, R. J.; Lu, Z. B.; Cammidge, A. N. Cyano substituted triphenylene-based discotic mesogens. *Liq. Cryst.* **1999**, *26*, 495−499.
(14) Praefcke, K.; Eckert, A.; Blunk, D. Liquid crystalline compounds. Part 105. Core-halogenated, helical-chiral triphenylene-based columnar liquid crystals. *Liq. Cryst.* **1997**, *22*, 113−119.
(15) Boden, N.; Bushby, R. J.; Cammidge, A. N.; Duckworth, S.; Headdock, G. α-Halogenation of triphenylene-based discotic liquid crystals: towards a chiral nucleus. *J. Mater. Chem.* **1997**, *7*, 601−605.
(16) Boden, N.; Bushby, R. J.; Cammidge, A. N.; Headdock, G. Versatile synthesis of unsymmetrically substituted triphenylenes. *Synthesis* **1995**, *1995*, 31−32.
(17) Kumar, S.; Manickam, M.; Varshney, S. K.; Rao, D. S. S.; Prasad, S. K. Novel heptasubstituted triphenylene discotic liquid crystals. *J. Mater. Chem.* **2000**, *10*, 2483−2489.
(18) Kumar, S.; Varshney, S. K. A new form of discotic metallomesogens: the synthesis of metal-bridged triphenylene discotic dimers. *Liq. Cryst.* **2001**, *28*, 161−163.
(19) Cammidge, A. N.; Gopee, H. Macrodiscotic triphenylenophthalocyanines. *Chem. Commun.* **2002**, 966−967.
(20) Schulte, J. L.; Laschat, S.; Schulte-Ladbeck, R.; von Arnim, V.; Schneider, A.; Finkelmann, H. Preparation of (η^6-alkoxytriphenylene)-tricarbonyl chromium(0) complexes: Mesomorphic properties of a disk-shaped chromium−arene complex. *J. Organomet. Chem.* **1998**, *552*, 171−176.
(21) Mohr, B.; Wegner, G.; Ohta, K. Synthesis of triphenylene-based porphyrazinato metal(II) complexes which display discotic columnar mesomorphism. *J. Chem. Soc., Chem. Commun.* **1995**, 995−996.
(22) Shi, J.; Wang, Y.; Xiao, M.; Zhong, P.; Liu, Y.; Tan, H.; Zhu, M.; Zhu, W. Luminescent metallomesogens based on platinum complex containing triphenylene unit. *Tetrahedron.* **2015**, *71*, 463−469.
(23) Yang, F.; Bai, X.; Guo, H.; Li, C. Ion complexation-induced mesomorphic conversion between two columnar phases of novel symmetrical triads of triphenylene-calix[4]arene-triphenylenes. *Tetrahedron Lett.* **2013**, *54*, 409−413.
(24) Chico, R.; Domínguez, C.; Donnio, B.; Heinrich, B.; Coco, S.; Espinet, P. Isocyano-Triphenylene Complexes of Gold, Copper, Silver, and Platinum. Coordination Features and Mesomorphic Behavior. *Cryst. Growth Des.* **2016**, *16*, 6984−6991.
(25) Kumar, S. Triphenylene-based discotic liquid crystal dimers, oligomers and polymers. *Liq. Cryst.* **2005**, *32*, 1089−1113.
(26) Gupta, S. P.; Gupta, M.; Pal, S. K. Highly Resolved Morphology of Room-Temperature Columnar Liquid Crystals Derived from Triphenylene and Multialkynylbenzene Using Reconstructed Electron Density Maps. *ChemistrySelect* **2017**, *2*, 6070−6077.
(27) Beltrán, E.; Garzoni, M.; Feringán, B.; Vancheri, A.; Barberá, J.; Serrano, J. L.; Pavan, G. M.; Giménez, R.; Sierra, T. Self-organization of star-shaped columnar liquid crystals with a coaxial nanophase segregation revealed by a combined experimental and simulation approach. *Chem. Commun.* **2015**, *51*, 1811−1814.
(28) Xiao, Y.; Su, X.; Sosa-Vargas, L.; Lacaze, E.; Heinrich, B.; Donnio, B.; Kreher, D.; Mathevet, F.; Attias, A. J. Chemical engineering of donor−acceptor liquid crystalline dyads and triads for the controlled nanostructuration of organic semiconductors. *CrystEngComm.* **2016**, *18*, 4787−4798.
(29) Feringán, B.; Romero, P.; Serrano, J. L.; Folcia, C. L.; Etxebarria, J.; Ortega, J.; Termine, R.; Golemme, A.; Giménez, R.; Sierra, T. H-Bonded Donor−Acceptor Units Segregated in Coaxial Columnar Assemblies: Toward High Mobility Ambipolar Organic Semiconductors. Segregated Donor−Acceptor Columns in Liquid Crystals That Exhibit Highly Efficient Ambipolar Charge Transport. *J. Am. Chem. Soc.* **2016**, *138*, 12511−12518.
(30) Hayashi, H.; Nihashi, W.; Umeyama, T.; Matano, Y.; Seki, S.; Shimizu, Y.; Imahori, H. Segregated Donor−Acceptor Columns in Liquid Crystals That Exhibit Highly Efficient Ambipolar Charge Transport. *J. Am. Chem. Soc.* **2011**, *133*, 10736−10739.
(31) Zhao, K. Q.; An, L. L.; Zhang, X. B.; Yu, W. H.; Hu, P.; Wang, B. Q.; Xu, J.; Zeng, Q. D.; Monobe, H.; Shimizu, Y.; Heinrich, B.; Donnio, B. Highly Segregated Lamello-Columnar Mesophase Organizations and Fast Charge Carrier Mobility in New Discotic Donor−Acceptor Triads. *Chem.—Eur. J.* **2015**, *21*, 10379−10390.
(32) Kira, A.; Umeyama, T.; Matano, Y.; Yoshida, K.; Isoda, S.; Park, J. K.; Kim, D.; Imahori, H. Supramolecular Donor−Acceptor Heterojunctions by Vectorial Stepwise Assembly of Porphyrins and Coordination-Bonded Fullerene Arrays for Photocurrent Generation. *J. Am. Chem. Soc.* **2009**, *131*, 3198−3200.
(33) Umeyama, T.; Tezuka, N.; Kawashima, F.; Seki, S.; Matano, Y.; Nakao, Y.; Shishido, T.; Nishi, M.; Hirao, K.; Lehtivuori, H.; Tkachenko, N. V.; Lemmetyinen, H.; Imahori, H. Carbon Nanotube Wiring of Donor−Acceptor Nanograins by Self-Assembly and Efficient Charge Transport. *Angew. Chem., Int. Ed.* **2011**, *50*, 4615−4619.
(34) Tritto, E.; Chico, R.; Sanz-Enguita, G.; Folcia, C. L.; Ortega, J.; Coco, S.; Espinet, P. Alignment of Palladium Complexes into Columnar Liquid Crystals Driven by Peripheral Triphenylene Substituents. *Inorg. Chem.* **2014**, *53*, 3449−3455.
(35) Miguel-Coello, A. B.; Bardají, M.; Coco, S.; Donnio, B.; Heinrich, B.; Espinet, P. Triphenylene-Imidazolium Salts and Their NHC Metal Complexes, Materials with Segregated Multicolumnar Mesophases. *Inorg. Chem.* **2018**, *57*, 4359−4369.
(36) Tritto, E.; Chico, R.; Ortega, J.; Folcia, C. L.; Etxebarria, J.; Coco, S.; Espinet, P. Synergistic π−π and Pt−Pt interactions in luminescent hybrid inorganic/organic dual columnar liquid crystals. *J. Mater. Chem. C* **2015**, *3*, 9385−9392.
(37) Chico, R.; de Domingo, E.; Domínguez, C.; Donnio, B.; Heinrich, B.; Termine, R.; Golemme, A.; Coco, S.; Espinet, P. High One-Dimensional Charge Mobility in Semiconducting Columnar Mesophases of Isocyano-Triphenylene Metal Complexes. *Chem. Mater.* **2017**, *29*, 7587−7595.
(38) De Domingo, E.; Folcia, C. L.; Ortega, J.; Etxebarria, J.; Termine, R.; Golemme, A.; Coco, S.; Espinet, P. Striking Increase in Hole Mobility upon Metal Coordination to Triphenylene Schiff Base Semiconducting Multicolumnar Mesophases. *Inorg. Chem.* **2020**, *59*, 10482−10491.
(39) Barcenilla, M.; Baena, M. J.; Donnio, B.; Heinrich, B.; Gutiérrez, L.; Coco, S.; Espinet, P. Triphenylene-ethylammonium tetrachlorometallate salts: multicolumnar mesophases, thermochromism and Langmuir films. *J. Mater. Chem. C* **2022**, *10*, 9222−9231.
(40) Conejo-Rodriguez, V.; Donnio, B.; Heinrich, B.; Termine, R.; Golemme, A.; Espinet, P. Mesogenic [Rh(L)4](A) complexes form mesophases with RhI—RhI-containing and triphenylene-discotic segregated columns. Effect of RhI—RhI interactions and A^- = $[Au(CN)_2]^-$ on hole mobility. *J. Mater. Chem. C* **2023**, *11*, 1435−1447.
(41) Reczek, J. J.; Villazor, K. R.; Lynch, V.; Swager, T. M.; Iverson, B. L. Tunable Columnar Mesophases Utilizing C_2 Symmetric Aromatic Donor-Acceptor Complexes. *J. Am. Chem. Soc.* **2006**, *128*, 7995−8002.
(42) Park, L. Y.; Hamilton, D. G.; McGehee, E. A.; McMenimen, K. A. Complementary C_3-Symmetric Donor-Acceptor Components: Cocrystal Structure and Control of Mesophase Stability. *J. Am. Chem. Soc.* **2003**, *125*, 10586−10590.
(43) Alvey, P. M.; Reczek, J. J.; Lynch, V.; Iverson, B. L. A Systematic Study of Thermochromic Aromatic Donor−Acceptor Materials. *J. Org. Chem.* **2010**, *75*, 7682−7690.
(44) Leight, K. R.; Esarey, B. E.; Murray, A. E.; Reczek, J. J. Predictable Tuning of Absorption Properties in Modular Aromatic Donor−Acceptor Liquid Crystals. *Chem. Mater.* **2012**, *24*, 3318−3328.

https://doi.org/10.1021/acs.cgd.3c00660
Cryst. Growth Des. 2023, 23, 6812−6821

(45) Delgado, M. C. R.; Kim, E. G.; da Silva Filho, D. A.; Bredas, J. L. Tuning the Charge-Transport Parameters of Perylene Diimide Single Crystals via End and/or Core Functionalization: A Density Functional Theory Investigation. *J. Am. Chem. Soc.* **2010**, *132*, 3375−3387.
(46) Kishore, R. S. K.; Kel, O.; Banerji, N.; Emery, D.; Bollot, G.; Mareda, J.; Gomez-Casado, A.; Jonkheijm, P.; Huskens, J.; Maroni, P.; Borkovec, M.; Vauthey, E.; Sakai, N.; Matile, S. Ordered and Oriented Supramolecular n/p-Heterojunction Surface Architectures: Completion of the Primary Color Collection. *J. Am. Chem. Soc.* **2009**, *131*, 11106−11116.
(47) Jones, B.; Facchetti, A.; Wasielewski, M. R.; Marks, T. J. Tuning Orbital Energetics in Arylene Diimide Semiconductors. Materials Design for Ambient Stability of n-Type Charge Transport. *J. Am. Chem. Soc.* **2007**, *129*, 15259−15278.
(48) Klivansky, L. M.; Hanifi, D.; Koshkakaryan, G.; Holycross, D. R.; Gorski, E. K.; Wu, Q.; Chai, M.; Liu, Y. A complementary disk-shaped π electron donor−acceptor pair with high binding affinity. *Chem. Sci.* **2012**, *3*, 2009−2014.
(49) Li, Y.; Li, M.-G.; Su, Y.-J.; Liu, J.-G.; Han, Y.-C.; Zheng, S.-J. Room temperature homeotropic alignment of mixed-stacking columns of H6TP donors and PDI acceptors by charge transfer interactions and size match. *J. Mol. Liq.* **2016**, *224* (A), 721−729.
(50) Eran, B. B.; Singer, D.; Praefcke, K. Disc-Like Chiral Palladium and Platinum Complexes: Synthesis and Mesomorphic Properties. *Eur. J. Inorg. Chem.* **2001**, *2001*, 111−116.
(51) Date, R. W.; Bruce, D. W. Discotic salicylaldimato metal complexes exhibiting columnar mesophases and their mixtures with rod-like salicylaldimato complexes. *Liq. Cryst.* **2004**, *31*, 1435−1444.
(52) Lee, C. K.; Peng, H. H.; Lin, I. J. B. Liquid Crystals of *N*,*N*^{c}-Dialkylimidazolium Salts Comprising Palladium(II) and Copper(II) Ions. *Chem. Mater.* **2004**, *16*, 530−536.
(53) Rourke, J. P.; Fanizzi, F. P.; Salt, N. J. S.; Bruce, D. W.; Dunmur, D. A.; Maitlis, P. M. *trans*-(η^2-Alkene)(4′-alkyloxy-4-stilbazole)dichloroplatinum; low melting organometallic mesogens. *J. Chem. Soc. Chem. Commun.* **1990**, 229−231.
(54) Ballesteros, B.; Coco, S.; Espinet, P. Mesomorphic Mixtures of Metal Isocyanide Complexes, Including Smectic C Mesophases at Room Temperature and Liquid Crystalline "Molecular Alloys. *Chem. Mater.* **2004**, *16*, 2062−2067.
(55) Allenbaugh, R. J.; Schauer, C. K.; Josey, A.; Martin, J. D.; Anokhin, D. V.; Ivanov, D. A. Effect of Axial Interactions on the Formation of Mesophases: Comparison of the Phase Behavior of Dialkyl 2,2′-bipyridyl-4,4′-dicarboxylate Complexes of Pt(II), Pt(IV), and Pt(II)/Pt(IV) Molecular Alloys. *Chem. Mater.* **2012**, *24*, 4517−4530.
(56) Cheda, J. A. R.; Ortega, F.; Sanchez Arenas, A.; Cosio, A.; Fernandez-Garcia, M.; Fernandez-Martin, F.; Roux, M. V.; Turrion, C. Binary phase diagrams of lead(II) n-alkanoates and n-alkanoic acids. *Pure Appl. Chem.* **1992**, *64*, 65−71.
(57) Seghrouchni, R.; Skoulios, A. Columnar to Nematic Mesophase Transition: Binary Mixtures of Copper Soaps with Hydrocarbons. *J. Phys. II France* **1995**, *5*, 1385−1405.
(58) Baxter, D. V.; Chisholm, M. H.; Lynn, M. A.; Putilina, E. F.; Trzaska, S. T.; Swager, T. Studies of Thermotropic Properties and the Mesophase of Mixtures of *n*-Alkanoates and Perfluoro-*n*-alkanoates of Dimolybdenum (M—M). *Chem. Mater.* **1998**, *10*, 1758−1763.
(59) Jongen, L.; Hinz, D.; Meyer, G.; Binnemans, K. Induced Mesophases in Binary Mixtures of Lanthanide(III) Dodecanoates. *Chem. Mater.* **2001**, *13*, 2243−2246.
(60) Inb-Elhaj, M.; Guillon, D.; Skoulios, A.; Maldivi, P.; Giroud-Godquin, A. M.; Marchon, J.-C. The structures of the crystalline phase and columnar mesophase of rhodium (II) heptanoate and of its binary mixture with copper (II) heptanoate probed by EXAFS. *J. Phys. II France* **1992**, *2*, 2237−2253.
(61) Folcia, C. L.; Alonso, I.; Ortega, J.; Etxebarria, J.; Pintre, I. C.; Ros, M. B. Achiral Bent-Core Liquid Crystals with Azo and Azoxy Linkages: Structural and Nonlinear Optical Properties and Photoisomerization. *Chem. Mater.* **2006**, *18*, 4617−4626.
(62) Tzeng, B. C.; Chan, S. C.; Chan, M. C. W.; Che, C. M.; Cheung, K. K.; Peng, S. M. Palladium(II) and Platinum(II) Analogues of Luminescent Diimine Triangulo Complexes Supported by Triply Bridging Sulfide Ligands: Structural and Spectroscopic Comparisons. *Inorg. Chem.* **2001**, *40*, 6699−6704.
(63) Thordarson, P. http://supramolecular.org.
(64) Howe, E. N. W.; Bhadbhade, M.; Thordarson, P. Cooperativity and Complexity in the Binding of Anions and Cations to a Tetratopic Ion-Pair Host. *J. Am. Chem. Soc.* **2014**, *136*, 7505−7516.
(65) Hibbert, D. H.; Thordarson, P. The death of the Job plot, transparency, open science and online tools, uncertainty estimation methods and other developments in supramolecular chemistry data analysis. *Chem. Commun.* **2016**, *52*, 12792−12805.
(66) Bannwarth, C.; Ehlert, S.; Grimme, S. GFN2-xTB—An Accurate and Broadly Parametrized Self-Consistent Tight-Binding Quantum Chemical Method with Multipole Electrostatics and Density-Dependent Dispersion Contributions. *J. Chem. Theory Comput.* **2019**, *15*, 1652−1671.
(67) Johnson, E. R.; Keinan, S.; Mori-Sánchez, P.; Contreras-García, J.; Cohen, A. J.; Yang, W. Revealing Noncovalent Interactions. *J. Am. Chem. Soc.* **2010**, *132*, 6498−6505.

https://doi.org/10.1021/acs.cgd.3c00660
Cryst. Growth Des. 2023, 23, 6812−6821